Estimation of Bubble Size Distribution Based on Power Spectrum

Jarmo Ilonen[1], Tuomas Eerola[1], Heikki Mutikainen[2], Lasse Lensu[1], Jari Käyhkö[2], and Heikki Kälviäinen[1]

[1] Machine Vision and Pattern Recognition Laboratory (MVPR), Lappeenranta University of Technology (LUT), Finland
[2] FiberLaboratory, Mikkeli University of Applied Sciences, Finland

Abstract. A bubble size distribution gives relevant insight into mixing processes where gas-liquid phases are present. The distribution estimation is challenging since accurate bubble detection from images captured from industrial processes is a complicated task due to varying lighting conditions which change the appearance of bubbles considerably. In this paper, we propose a new method for estimating the bubble size distribution based on the image power spectrum. The method works by calculating the power spectrum for a number of frequency bins and learning the linear relationship between the power spectrum and the bubble size distribution. Since the detection of individual bubbles is not needed, the proposed method is remarkably faster than the traditional approaches. The method was compared to a geometry-based bubble detection method with both synthetic and industrial image data. The proposed method outperformed the bubble detection based approach especially in the cases where bubbles were small and the number of bubbles high.

1 Introduction

This paper focuses on estimating the size distribution of bubbles, or more generally, transparent approximately spherical objects in a liquid. The research is driven by the pulpmaking industry, in particular the development of the pulp delignification process. Pulp delignification with oxygen is a very energy-intensive operation. To optimize and control the process, it is essential to be able to characterize the process, especially the sizes of the oxygen bubbles. The recent progress in camera and illumination technologies has made it possible to capture images inside the process machines. In [11] an imaging setup applied to the pulp mill environment was presented. From the produced images an expert could determine the bubble size distribution by manually marking the bubbles. However, manual analysis of the images is very time-consuming, motivating the development of automatic methods for estimating the bubble size distribution.

The typical approach to estimate the bubble size distribution is to first detect and segment the bubbles, and to compute the size of each detected bubble separately [13]. The bubble detection problem is not easy to solve because the bubbles are transparent and the illumination conditions are challenging when

E. Bayro-Corrochano and E. Hancock (Eds.): CIARP 2014, LNCS 8827, pp. 38–45, 2014.

imaging inside an industrial process, which causes the bubble appearance to vary. In the images, bubbles appear as roughly circular objects which motivates to solve the problem as the detection of circles. Two common approaches are used to detect circular objects: geometry-based and appearance-based approaches. In the geometry-based approach a circular model parameterized by its center and radius is fitted to the image edge map. These methods typically utilize a voting technique, such as the Hough Transform (HT) [4] or its modifications [9]. The geometry-based approaches suffer from a large number of false positives and are sensitive to noise. Moreover, they often fail to detect small blob-like bubbles that do not have a ridge edge expected by the model [13]. The appearance-based approach uses typically a sliding window where a template of the object of interest and the grayscale image are convolved. The template matching techniques are difficult to apply for the bubble detection since the bubbles may appear differently depending on the bubble location in the image and lighting.

Typical images from a real industrial process contain a huge amount of bubbles and have a low image quality because of harsh conditions (see Fig. 1). Detecting each individual bubble, which can overlap because of their transparent nature, is difficult and also time consuming. In this work, we propose a novel power spectrum based method to estimate the bubble size distribution directly from the images. This makes the detection of bubbles unnecessary and, therefore, the problems mentioned above can be avoided. The method is validated with both synthetic and novel image data from a real industrial environment.

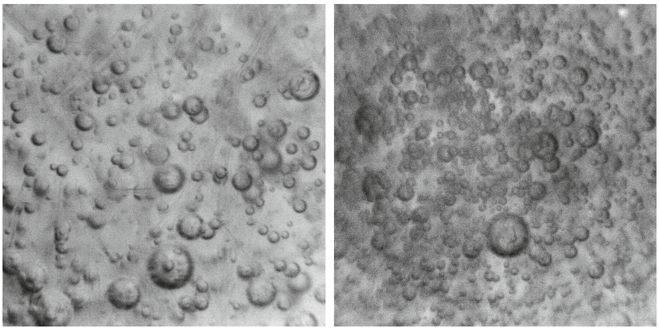

(a) (b)

Fig. 1. Examples of pulp suspension images with different process variables: (a) 1000 rpm; (b) 1380 rpm

2 Related Work

Image power spectrum has been a popular tool for texture analysis or discrimination [6,7,10]. In texture analysis, local power spectrum, often implemented using Gabor filters, is used to be able to discriminate between different textures in the different parts of an image. In our case, we are not interested in the local power spectrum, but instead the power spectrum of the whole image. The global power spectrum has been used in [12] to classificy real-world images, for example, whether the scene is natural or artificial (man-made). Other applications have been the visual quality estimation of transmitted images without having the reference image [14] and the detection of hidden messages in images [1].

A method for determining bubble size distribution has been presented in [5,8]. The method requires a binary image where the bubbles and background are separated. In our case with images from the industrial process (Fig. 1) that would be very difficult to do with sufficient quality. Therefore, as the reference method we use the bubble detection method based on concentric circular arrangements (CCA) [13] developed particularly for pulp suspension images. It has been shown to achieve good performance in the given task when the amount of bubbles is reasonable. The main problem of the method is the low detection rate of small blob-like bubbles with no ridge edge.

3 The Estimation Method

The method presented here for estimating the bubble count or volume distribution works in the frequency domain and uses the power spectrum of the image [2]. Fourier transform of two signals (here bubbles) is the same as taking the Fourier transform for them separately and adding them up. Therefore, the Fourier transform of an image consisting of bubbles is the same as Fourier transforms of images of separate bubbles. However, the power spectrum of two combined signals is not the same as their separate power spectra combined because the phase (location) difference can even cause them to nullify each other. In the case of a large set of bubbles located randomly it is reasonable that their phases overlap predictably on average so that the distribution can still be determined with a good accuracy from the power spectrum.

The method consists of the following steps:

1. Calculate the power spectrum of an image using L frequency bands.
2. Use principal component analysis (PCA) to reduce the data to M dimensions.
3. Use multivariate linear regression to learn the dependency between the power spectrum and bubble count or volume distribution.

The power spectrum is a vector of the portion of a signal power falling into specified frequency bins. It is acquired by applying 2-D discrete Fourier transform to the signal (image) and computing the energy belonging to L linearly spaced frequency bins, producing a vector P_i for an image i. The frequency range is limited at the lower end because we have knowledge of the maximum size of the bubbles, and therefore, the lowest possible frequencies caused by actual bubbles.

To reduce the dimensionality, principal component analysis (PCA) is used. The principal components are calculated from the matrix containing power spectra of N images, $P_i, i = [1 \ldots N]$. The M principal components can then be used to reduce the dimensionality of the original power spectrum P_i to p_i which is a vector with M components.

Multivariate linear regression [3] is used to find out the relationship between vector p_i and the bubble count or volume distribution D_i in the image (example in Fig. 2). The distributions used are histograms with K bins, with $K = 10$ in the example and all experiments. The multivariate linear regression is defined as

$$\begin{pmatrix} D_{1,1} & \dots & D_{1,K} \\ & \vdots & \\ D_{N,1} & \dots & D_{N,K} \end{pmatrix} = \begin{pmatrix} p_{1,1} & \dots & p_{1,M} & 1 \\ & \vdots & & 1 \\ p_{N,1} & \dots & p_{N,M} & 1 \end{pmatrix} \mathbf{X} + \epsilon \tag{1}$$

where $\mathbf{X}$ is the $M + 1 \times K$ matrix to be estimated and ϵ is the noise term. $\mathbf{X}$ is solved as a linear least squares estimation problem. The distribution D_j for a new image j can be estimated by calculating the power spectrum P_j, using PCA to reduce its dimensionality and getting p_j and then

$$D_j = (p_{j,1} \dots p_{j,M} 1)\, \mathbf{X}. \tag{2}$$

4 Experiments

In all experiments, the power spectrum was calculated from 19 linearly spaced frequency bins, $f = [0.05, 0.5]$, and dimensionality was reduced with PCA to 5.

Synthetic Data. To properly evaluate the method performance, a ground truth is needed for either the spatial locations and sizes of the bubbles, or at least their size distribution. Taking into account the nature of the real image data producing either one accurately for a large number of images is infeasible. Therefore, synthetic image data was used to study the methods in detail.

Example synthetic images and bubble size distribution histograms can be seen in Fig. 2. In the first case with a low number of bubbles, Fig. 2a, the CCA method found all bubbles except for some of the smallest one. Some false positives are caused by detectiong being in slightly wrong location or too large. In general, the bubble size distribution histograms by both number and volume are close to the ground truth and the differences are caused by not detecting some of the smallest bubbles and overestimating the size for some of the others. The power spectrum based method gives a better estimate for the number of bubbles, but in the volume histogram it cannot detect the "spikes" caused by large bubbles and gives a smoother distribution than the ground truth.

In the example with more bubbles, Fig. 2(b), CCA missed the majority of the small bubbles and the false detection of one large bubble (top middle) caused a large discrepancy in the bubble volume histogram. With the power spectrum based method the number of bubbles is very close to the true distribution. The volume estimate is not as accurate, but the general shape of the distribution is relatively close to true.

For the next experiment, a synthetic time series data set with 1200 images was generated. The data set mimics the properties of real images of the dispersion process where the bubble distribution is affected by the rotor speed: with high rpm, the bubble size distribution changes so that the number of small bubbles

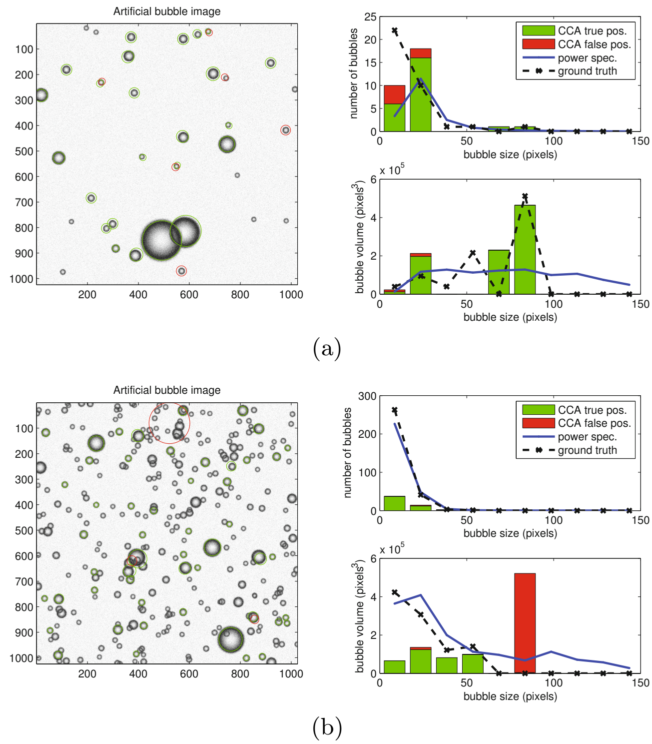

Fig. 2. Examples of synthetic bubble image and bubbles detected by the CCA method (left) and bubble size distribution histograms (right): (a) 35 bubbles; (b) 300 bubbles

increases and large bubbles become rare. The synthetic data set imitates this effect of increasing the rotor speed. Each image in the set is independent in the sense that the same bubbles do not move between images; every image is randomly generated. Two images from the sequence can be seen in Figs. 2a (98th image) and 2b (877th image).

Fig. 3 shows the ground truth and the estimated total number and total volume of bubbles. All results are presented as the average of 20 images to remove high variations between single images. The power spectrum based method follows the true number of bubbles very accurately through the series. For the total volume, the ground truth includes more variations caused by large individual bubbles than the power spectrum estimates. CCA starts well with the low bubble count, but as the bubble count increases, it cannot detect the majority of the bubbles and the volume estimate even decreases during the series.

The mean absolute errors in the detected bubble count and volume histograms are shown in Fig. 3(c-d). In this case, not only the total number and total volume have to match, but also their distribution. For the number of bubbles, the power spectrum based method gives very accurate distributions for the whole time series, but CCA suffers from not being able to detect small bubbles when their

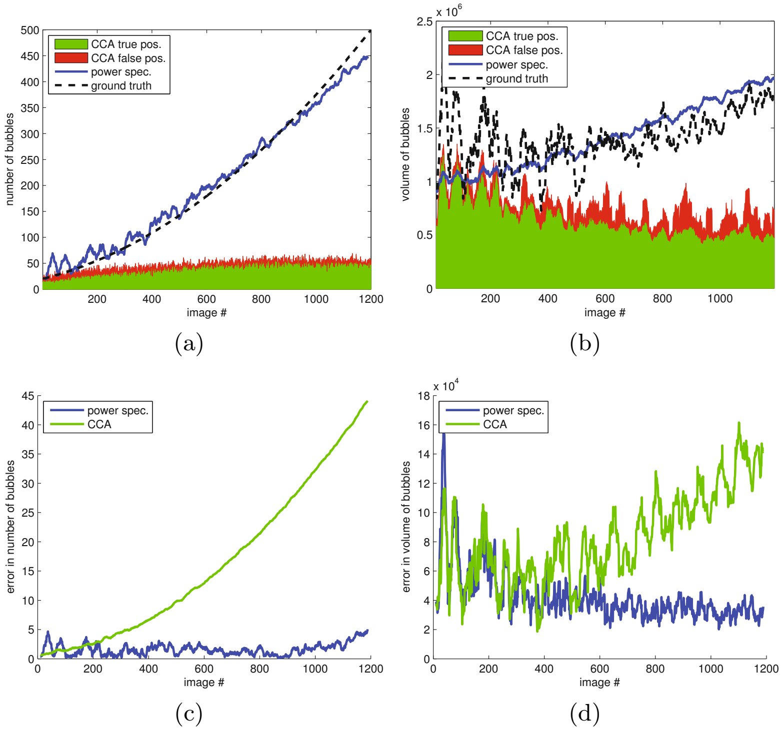

Fig. 3. Experiments with the synthetic time series data set: (a) Total number of bubbles; (b) Total volume of bubbles; (c) Mean absolute errors in total number of bubbles; (d) Mean absolute errors in total volume of bubbles.

number increases. For the volume histogram, CCA starts slightly better than the power spectrum based method because it can detect large individual bubbles present in the early images, but later on the power spectrum based method performs better.

Real Data. A trial session was performed in a softwood kraft pulp mill. Images were gathered from the oxygen delignification process of a pulp fiber line. The used imaging setup consisted of an AVT Guppy Pro F-503B camera with a picture size of 2588 × 1940 pixels, a Richard Wolf 51 camera adapter and a Richard Wolf borescope. A Cavitar Cavilux Smart pulsed diode laser light source was used for illumination. The experiments were performed with varied mixer rotor speeds from 900 rpm to 1380 rpm (see examples in Fig. 1). All other process variables were kept constant during the trial session. The imaging setup was used in two locations of the pulp fiber line. In each location, 10 images were captured with every used rotor speed, and for them the ground truth (bubble locations and sizes) were manually marked. Only the central 1482 × 1482 portions of the images were used.

The results with the real data are presented in Fig. 4. As with the synthetic data and the low rotor speed, CCA works well. When the speed is increased and the bubble size distribution starts to favor small bubbles, however, its detection performance suffers. The power spectrum based method can capture the true distribution much better with high speeds.

The average computation time for the MATLAB implementation of the power spectrum based method was $0.6s$ per image while the CCA method took $5.1s$ with a computer equipped with Intel Core i5 processor running at $3.4GHz$. A much faster implementation of the power spectrum method could be made because currently most of the time is wasted in various overheads and not on the only computationally intensive operation, fast Fourier transform. This makes the power spectrum based method more suitable for the industrial process control systems where real-time performance is required.

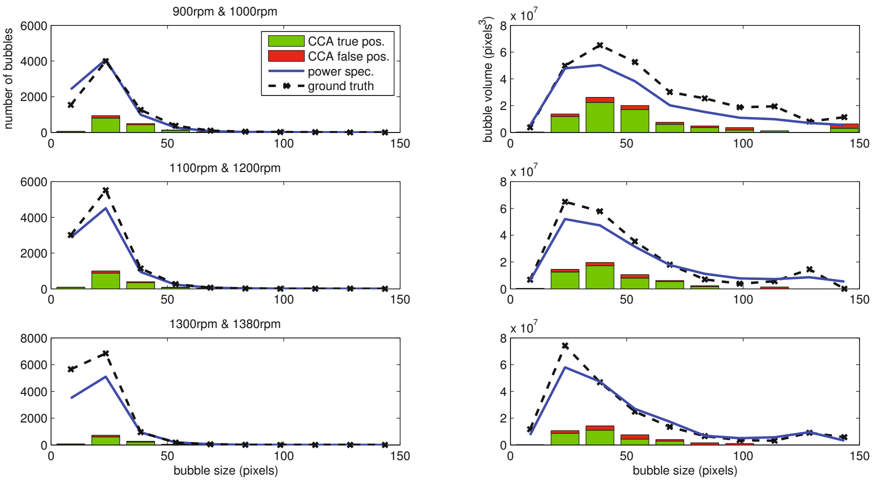

Fig. 4. Bubble count and volume distributions with real data

5 Conclusions

In this paper, a new method for estimating the bubble size distribution was proposed. The method is based on the image power spectrum and it was compared to a geometry-based bubble detection method (CCA) with both synthetic and industrial image data. In the experiments, the performance of the estimation method was evaluated using synthetic time series data which mimics the effect of increasing mixer rotor speed. The estimation method could detect the changing bubble size distribution well, while the reference method struggled when there was a large number of bubbles. Similar results were obtained with the real data. In the future the method could be used directly to classify the state of the dispersion, i.e., is it good or if some process parameter should be changed. This, however, is a new area for the pulp industry and requires further study of dispersion in oxygen delignification process.

Acknowledgments. The research was supported by the PulpVision EU TEKES 70010/10 and 70040/11 projects.

References

1. Amin, P., Subbalakshmi, K.P.: Detecting hidden messages using image power spectrum. In: IEEE Int. Conf. on Image Processing, vol. 1, pp. 421–424 (2007)
2. Bracewell, R.: Fourier Analysis and Imaging. Springer US (2003)
3. Christensen, R.: Plane Answers to Complex Questions: The Theory of Linear Models. Springer (2011)
4. Duda, R.O., Hart, P.E.: Using the hough transform to detect lines and curves in pictures. Communications of the ACM 15, 11–15 (1972)
5. Emery, X., Kracht, W., Egaña, Á., Garrido, F.: Using two-point set statistics to estimate the diameter distribution in boolean models with circular grains. Mathematical Geosciences 44(7), 805–822 (2012)
6. Fogel, I., Sagi, D.: Gabor filters as texture discriminator. Biological Cybernetics 61(2), 103–113 (1989)
7. Grigorescu, S., Petkov, N., Kruizinga, P.: Comparison of texture features based on gabor filters. IEEE Transactions on Image Processing 11(10), 1160–1167 (2002)
8. Kracht, W., Emery, X., Paredes, C.: A stochastic approach for measuring bubble size distribution via image analysis. International Journal of Mineral Processing 121(10), 6–11 (2013)
9. Kyrki, V., Kälviäinen, H.: Combination of local and global line extraction. Journal of Real-Time Imaging JRTI 6(2), 79–91 (2000)
10. Liu, X., Wang, D.: Texture classification using spectral histograms. IEEE Transactions on Image Processing 12(6), 661–670 (2003)
11. Mutikainen, H., Peltonen, K., Tirri, T., Kayhko, J.: Characterisation of oxygen dispersion in mediumconsistency pulp mixing. Appita Journal 67(1), 37–42 (2014)
12. Oliva, A., Torralba, A.B., Guérin-Dugué, A., Hérault, J.: Global semantic classification of scenes using power spectrum templates. In: Int. Conf. on Challenge of Image Retrieval (1999)
13. Strokina, N., Matas, J., Eerola, T., Lensu, L., Kälviäinen, H.: Detection of bubbles as concentric circular arrangements. In: Int. Conf. on Pattern Recognition (2012)
14. Zhang, Y., An, P., Zhang, Q., Shen, L., Zhang, Z.: A no-reference image quality evaluation based on power spectrum. In: 3DTV Conference, pp. 1–4 (2011)